



## Photocatalytic Properties of Mixed-Crystalline Titanate Nanotubes Prepared by Hydrothermal Reaction

YANLI WANG, JIA WANG, QIUXIA WU, SHUN TAN, HUIJIAO GUO, MINGHONG WU and ZHENG JIAO\*

Institute of Nanochemistry and Nanobiology, School of Environmental and Chemical Engineering, Shanghai University, Shanghai 200444, P.R. China

\*Corresponding author: Tel/Fax: +86 21 66135275; E-mail: zjiao@shu.edu.cn

(Received: 19 June 2010;

Accepted: 2 March 2011)

AJC-9682

In this paper, mixed-crystalline titanate nanotubes ( $\text{TiO}_2$ -NTs) are grown by hydrothermal reaction in a 10M NaOH aqueous solution for the application in photocatalysis. The morphology and structure of prepared samples are characterized by XRD, SEM, TEM and BET.  $\text{TiO}_2$ -NTs have uniform shapes. XRD analysis indicates that the mainly phase are anatase  $\text{TiO}_2$  and rutile  $\text{TiO}_2$ . The photocatalytic properties of  $\text{TiO}_2$ -NTs were investigated. It is found that the  $\text{TiO}_2$ -NTs with mixed crystal structures exhibited improved photocatalytic activity in comparison with rutile  $\text{TiO}_2$  nanoparticle and the commercial Degussa P-25. The photocatalytic mechanism of  $\text{TiO}_2$ -NTs was also discussed.

**Key Words:** Titanate, Nanotubes, Photocatalytic activity.

### INTRODUCTION

In the past decade, many efforts have been taken on the semiconductor photocatalysts for their environmental applications in air purification, water disinfection and hazardous water remediation<sup>1-3</sup>. Titanium(IV) oxide has been extensively applied as a photocatalyst due to its high stability and semiconductor abilities capable of generating charge carriers by absorbing energy<sup>4</sup>. With the decrease of particle's size, the photocatalytic activity of titania increased dramatically, which is probably due to the significant particle-size effect and the large specific surface<sup>5-7</sup>.  $\text{TiO}_2$  nanoparticles with large surface area shows highly photocatalytic activity when it is used as a photocatalyst<sup>8-10</sup>. Recently, much effort has been directed at obtaining  $\text{TiO}_2$  nanotubes with a large surface area and high photocatalytic activity.  $\text{TiO}_2$  nanotubes with diameters of 70-100 nm were produced using the sol-gel method reported by Kasuga *et al.*<sup>11</sup>. High-purity nanotubes are formed depending on the treatment temperature and holding time<sup>12</sup>. Most of the titanium dioxide nanoparticles used as photocatalysts is single crystalline, but many researchers reported that the photocatalytic activity of anatase  $\text{TiO}_2$  can be improved by mixing other nanostructures, which is well-known by mixed crystal effect<sup>13</sup>. The frequently used high activity P-25 is a good example, which is composed of approximately 80 % anatase and 20 % rutile  $\text{TiO}_2$ <sup>14</sup>. In this paper, the titanate nanotubes ( $\text{TiO}_2$ -NTs) were grown by hydrothermal reaction.  $\text{TiO}_2$ -NTs have a good photocatalytic activity compared with rutile  $\text{TiO}_2$  nanoparticle

and P-25. The photocatalytic mechanism of the  $\text{TiO}_2$ -NTs was discussed based on experimental results.

### EXPERIMENTAL

**Preparation of titanate nanotubes:** All chemical reagents were analysis pure, supplied by Sinopharm Chemical Reagent Co. Ltd. The rutile  $\text{TiO}_2$  powder of 80-100 nm was provided by Professor Shi Liyi from Shanghai University (purity  $\geq 95\%$ , coated with  $\text{SiO}_2$ , water dissolvable).  $\text{TiO}_2$ -NTs were prepared as follows<sup>11</sup>: 200 mg  $\text{TiO}_2$  powder was added in 140 mL of 10M NaOH solution and ultrasonic dispersed for 0.5 h. The mixture was placed in a 200 mL Teflon-lined autoclave; the autoclave was heated to 150 °C for 35 h. After that, the mixtures were centrifuged at 8000 rpm. Precipitate were separated and washed with 0.5M HCl solution and distilled water several times until the pH of the rinsing solution reached 6.5. The washed precipitate was dried at 60 °C overnight to get  $\text{TiO}_2$  nanotube samples.

**Photocatalytic activity:** The photocatalytic activity of  $\text{TiO}_2$ -NTs was performed by measure the photocatalytic discolourization of methyl orange aqueous solution at ambient temperature using SGY-IB multifunctional photochemical reaction instrument (Stonetech Eec LTD., Nanjing). A 300 W high pressure mercury lamp was used to provide the ultraviolet light and a 350 W xenon lamp to simulate the visible light irradiation condition at room temperature.

## RESULTS AND DISCUSSION

The structure of TiO<sub>2</sub>-NTs was analyzed with a D/max-2550 X-ray diffraction (XRD). In Fig. 1 it can be found that main crystal structure is anatase, but still a certain amount rutile TiO<sub>2</sub> exists. It is reported that TiO<sub>2</sub> crystals become amorphous while treated in NaOH aqueous, because the Ti-O bond was broken and Ti-O-Na or Ti-OH bonds were arbitrarily formed. TiO<sub>2</sub>-NTs were generated after the treatment of TiO<sub>2</sub> crystals in acidic solution. Both rutile-type and anatase-type TiO<sub>2</sub> crystals can be used as starting material to subjected to hydrothermal treatment in NaOH aqueous<sup>11,15</sup>. Several characteristic peaks correspond to the crystal structure of H<sub>2</sub>Ti<sub>3</sub>O<sub>7</sub> (Na<sub>2</sub>Ti<sub>3</sub>O<sub>7</sub>) and Na<sub>x</sub>H<sub>2-x</sub>Ti<sub>3</sub>O<sub>7</sub> were also observed. By controlling the conditions of acid treatment, the amount of residual Na<sup>+</sup> ions changes and it is possible to form either titania or titanate nanotubes<sup>16</sup>. Depending on the conditions of the formation process and type of residual Na, several types of crystal, such as TiO<sub>2</sub>, H<sub>2</sub>Ti<sub>3</sub>O<sub>7</sub> and Na<sub>x</sub>H<sub>2-x</sub>Ti<sub>3</sub>O<sub>7</sub> were reported to be deposited<sup>17-19</sup>. After treated with 400 °C for 5 h, only TiO<sub>2</sub> nanotubes exists.

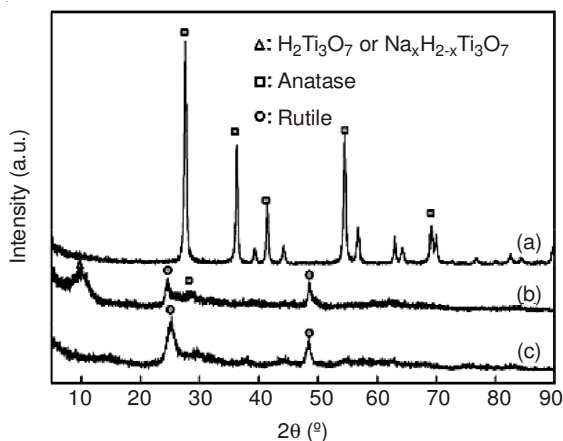


Fig. 1. X-Ray diffraction patterns for samples (a) the rutile-type TiO<sub>2</sub> nanoparticle. (b) titanate nanotubes obtained in the 10M NaOH aqueous for 35 h at 150 °C. (c) prepared titanate nanotubes after calcined for 5 h at 400 °C

The morphology of TiO<sub>2</sub>-NTs were observed by JEM-2010 transmission electron microscopy, results were shown in Fig. 2. It was reported that TiO<sub>2</sub>-NTs are formed by the curl of nanobelts<sup>3</sup>. In this paper, the morphology of nanotubes or nanobelts was substantially affected by changing the hydrothermal treatment temperature and holding time. At lower treating temperature 110 °C and shorter holding time about 15 h, the unreacted TiO<sub>2</sub> particles still exists (Fig. 2a). At higher temperature (170 °C) and prolonged duration (72 h), there are abundant nanobelts (Fig. 2b). Numerous nanotubes were found (Fig. 2c) when the powders were treated with 10M NaOH for 35 h at 150 °C. After being calcined at 400 °C for 5 h, TiO<sub>2</sub>-NTs had no obvious change except the length is comparatively shorter (Fig. 2d). The shape of the single TiO<sub>2</sub> nanotube was observed by Shimazu SPM-9600 atomic force microscopy and JSM-670 scanning electron microscopy (Jeol) (Fig. 3). TiO<sub>2</sub>-NTs has uniform inner and outer diameters along their length (Fig. 3a), a large amount of nanotubes had a narrow

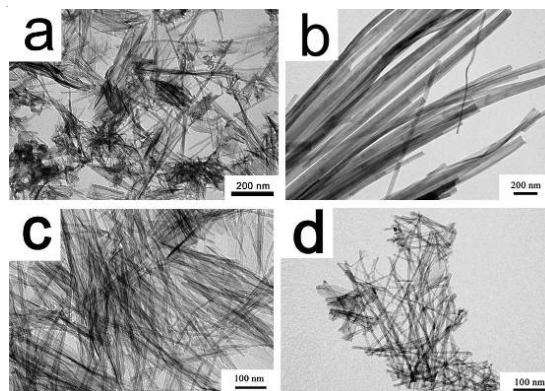
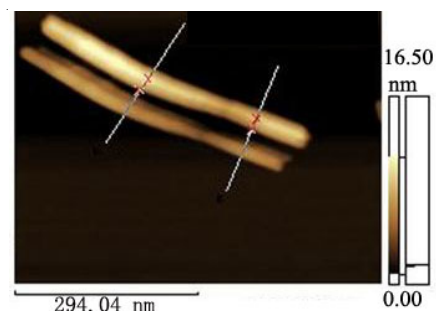
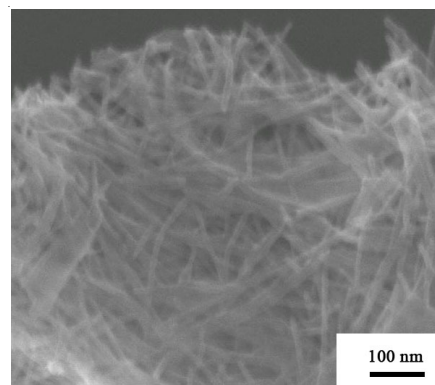


Fig. 2. TEM images of the TiO<sub>2</sub>-NTs. (a) 15 h at 110 °C; (b) 72 h at 170 °C; (c) 35 h at 150 °C; (d) calcined for 2 h



(a)



(b)

Fig. 3. SEM and AFM image of TiO<sub>2</sub>-NTs. (a) AFM image; (b) SEM image

size distribution with an average diameter of 4-5 nm and several hundreds nanometers in length (Fig. 3b). Specific surface areas of TiO<sub>2</sub>-NTs were measured in ASAP 2020M + C nitrogen adsorption apparatus (Micromeritics Instruments Company, USA). The nitrogen desorption/adsorption isotherms (Fig. 4) showed the TiO<sub>2</sub>-NTs have the type IV isotherm with type H<sub>3</sub> hysteresis loop according to BDDT classification with high BET surface area of 323 m<sup>2</sup>/g. The higher specific surface area of the nanotube is expected to enhance the photocatalytic activity of titanate nanotubes.

The photocatalytic activity of the TiO<sub>2</sub>-NTs was evaluated by photocatalytic oxidation of methyl orange aqueous solution. TiO<sub>2</sub>-NTs showed high photocatalytic activity in Fig. 5. Absorption peak gradually decreased with increasing irradiation time which indicates the relationships between photocatalytic activity of TiO<sub>2</sub>-NTs and irradiation time in different irradiation conditions.

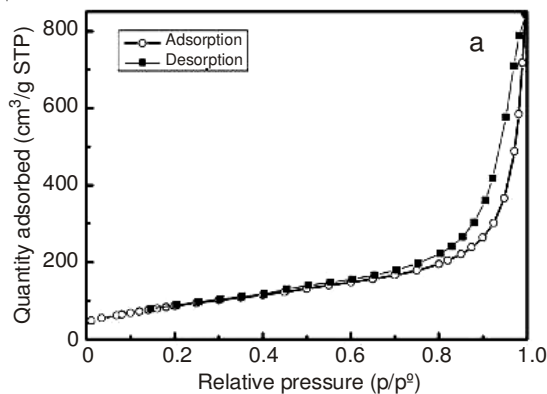


Fig. 4. Nitrogen adsorption-desorption isotherms of  $\text{TiO}_2$ -NTs

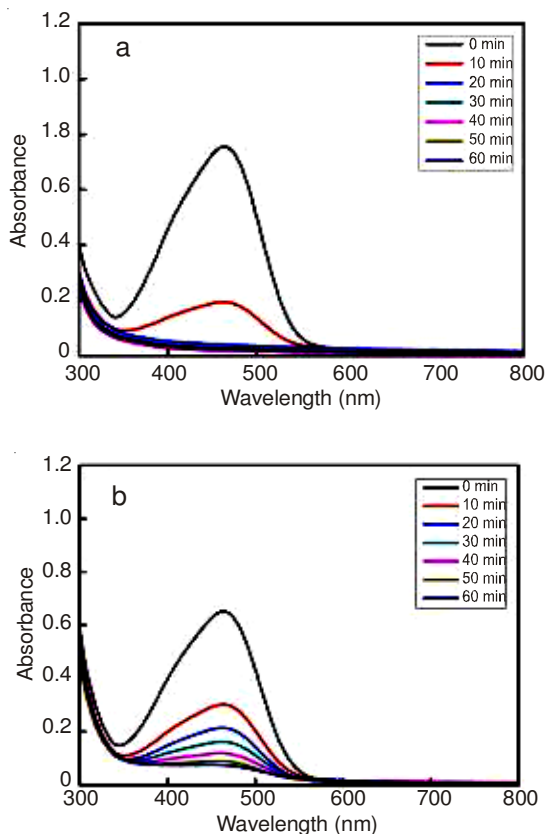


Fig. 5. Absorption spectra of the methyl orange aqueous solution (a) in UV irradiation conditions; (b) in visible light irradiation conditions

$\text{TiO}_2$ -NTs exhibited decent photocatalytic activity for the photocatalytic oxidation of methyl orange. Under the UV irradiation,  $\text{TiO}_2$ -NTs showed high photocatalytic activity. Concentration of the methyl orange decreased rapidly with increasing UV irradiation time. It is reported that the higher radiation energy was discharged, the more efficiency was degraded<sup>20</sup>. After UV irradiation without filter for 20 min, the absorption peak of the aqueous solution of methyl orange was very weak. Moreover, experimental observation indicated that the colour of the aqueous solution of methyl orange changed from orange to nearly transparent after UV irradiation for 20 min, indicating a nearly complete degradation of methyl orange<sup>21</sup>. By comparing the Fig. 5 (a) and (b), it is observed that the photocatalytic ability of  $\text{TiO}_2$ -NTs in the UV irradiation conditions is better than visible light irradiation.

For comparison, the photocatalytic activity of commercial photocatalyst P25 was also tested under identical conditions. Fig. 6 also shows that the relationships between  $C_t/C_0$  and photocatalytic reaction time under the different irradiation condition. From Fig. 6, it can be seen that photocatalytic degradation rates of the methyl orange decreased with the prolongation of the photocatalytic reaction time. The prepared samples have better photocatalytic effect than the commercially available Degussa P-25 in ultraviolet light exposure.  $\text{TiO}_2$ -NTs has large BET surface area of about  $323 \text{ m}^2/\text{g}$  and therefore shows an extremely high absorption capacity, which is beneficial to the collection of the organic pollute molecules like those of methyl orange. Under UV light irradiation, the methyl orange molecules absorbed on the surfaces of nanotubes and the produced electrons were transferred to  $\text{TiO}_2$ -NTs. Moreover, mixed-crystalline types play a crucial role in improving the photocatalytic activity of  $\text{TiO}_2$ -NTs.

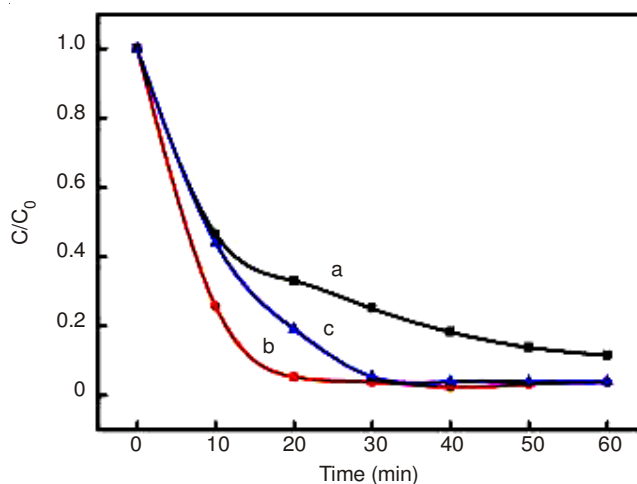


Fig. 6.  $(C_t/C_0)$  versus time curve for the methyl orange aqueous solution. (a)  $\text{TiO}_2$ -NTs as the photocatalyst: under visible light irradiation conditions; (b) under UV irradiation conditions; (c) the commercial photocatalyst P25 under UV irradiation conditions

## Conclusion

In summary, mixed-crystalline titanate nanotube were prepared through hydrothermal treatment by controlling the conditions of treatment. Compared with Degussa P25, a widely used commercial  $\text{TiO}_2$ ,  $\text{TiO}_2$ -NTs exhibited a much improved photocatalytic activity for the photocatalytic oxidation of methyl orange. This could be attributed to the fact that the former had larger specific surface area, higher pore volume and in the mixed-crystalline.

## ACKNOWLEDGEMENTS

The authors gratefully acknowledged the financial supports from the MOST 973 Program (2006CB705604), Shanghai Leading Academic Disciplines (S30109), Natural Science Foundation of China (20871081), Natural Science Foundation of Shanghai (08ZR1407800) and Innovation Program of Shanghai Municipal Education Commission (09YZ25).

## REFERENCES

1. H.G. Yu, J.G. Yu, B. Cheng and J. Lin, *J. Hazard. Mater.*, **147**, 581 (2007).
2. G.M. An, W.H. Ma, Z. Sun, Z.M. Liu, B.X. Han, S.D. Miao, Z.J. Miao and K.L. Ding *Carbon*, **45**, 1795 (2007).
3. G.H. Du, Q. Chen, R.C. Che, Z.Y. Yuan and L.-M. Peng, *Appl. Phys. Lett.*, **79**, 3702 (2001).
4. L.L. Costa and A.G.S. Prado, *J. Photochem. Photobiol. A: Chem.*, **201**, 45 (2009).
5. H. Oha, J. Lee and Y. Kim, *Appl. Catal. B: Environ.*, **144**, 142 (2008).
6. G. Guo, C. He and Z. Wang, F.-B. Gu and D.-M. Han *Talanta*, **72**, 1687 (2007).
7. M. Anpo and M. Takeuchi, *J. Catal.*, **216**, 505 (2003).
8. Y.H. Ao, J.J. Xu, D.G. Fu, L. Ba and C.W. Yuan *Nanotechnology*, **19**, 405604 (2008).
9. Y. Liu, J. Li, X. Qiu and C. Burda, *Water Sci. Technol.*, **54**, 47 (2006).
10. J.C. Yu, J. Yu and J. Zhao, *Appl. Catal. B: Environ.*, **36**, 31 (2002).
11. T. Kasuga, M. Hiramatsu, A. Hoson, T. Sekino and K. Niihara, *Langmuir*, **14**, 3160 (1998).
12. R. Ma, K. Fukuda, T. Sasaki, M. Osada and Y. Bando, *J. Phys. Chem. B*, **109**, 6210 (2005).
13. Y.Q. Wang, G.Q. Hu, X.F. Duan, H.L. Sun and Q.K. Xue, *Chem. Phys. Lett.*, **365**, 427 (2002).
14. Y. Yan, X. Qiu, H. Wang, L. Li, X. Fu, L. Wu and G. Li, *J. Alloys Comp.*, **460**, 491 (2008).
15. T. Kasuga, M. Hiramatsu, A. Hoson, T. Sekino and K. Niihara, *Adv. Mater.*, **15**, 1307 (1999).
16. T. Kasuga, *Thin Solid Films*, **496**, 141 (2006).
17. D.S. Seo, J.K. Lee and H. Kim, *J. Crystal Growth*, **229**, 428 (2001).
18. B.D. Yao, Y.F. Chan, X.Y. Zhang, W.F. Zhang, Z.Y. Yang and N. Wang *Appl. Phys. Lett.*, **82**, 281 (2003).
19. Q. Chen, G.H. Du, S. Zhang and L.-M. Peng, *Acta Crystallogr. B*, **58**, 587 (2002).
20. H. Xu, G. Vanamu, Z. Nie, H. Konishi, R. Yeredla, J. Phillips and Y. Wang, *J. Nanomater.*, Article ID 78902 (2006).
21. H. Li, B. Zhu and Y. Feng, S. Wang, S. Zhang and W. Huang, *J. Solid State Chem.*, **180**, 2136 (2007).

THIRD INTERNATIONAL CONFERENCE ON SCIENCE IN SOCIETY WASHINGTON DC

5 — 7 AUGUST, 2011

WASHINGTON DC, UNITED STATES

Contact:

Audrey LeGrande

Website: <http://science-society.com/conference-2011/>